articles

molecular pharmaceutics

Nucleobase- and p-Glycoprotein-Mediated Transport of AG337 in a Caco-2 Cell Culture Model

Ming Hu* and Jiyue Chen

Department of Pharmaceutical Sciences, College of Pharmacy, Washington State University, Pullman, Washington 99164-6534

Received September 24, 2003

Abstract: This study aimed to determine the intestinal transport characteristics of AG337. Caco-2 cell monolayers were used for directional transport of AG337. The results indicated that the rate of basolateral (BL) to apical (AP) or secretory transport of AG337 was always higher than the rate of AP to BL or absorptive transport. The BL−AP/AP−BL ratio increased from 7.6 to 17.2 as the concentration increased from 10 to 75 μM and stabilized afterward. The following results suggest that the p-glycoprotein is involved in the AP efflux of AG337. (1) Verapamil completely abolished the directional transport. (2) The apparent activation energy for secretory transport was high (33 kcal/mol). (3) Secretory transport was inhibited by verapamil (63%) and dipyridamole (35%), but not by probenecid. (4) AP to BL transport was enhanced by verapamil (232%) and dipyridamole (41%), but was not altered by probenecid or an AP pH change. An additional carrier mechanism may be involved in the AP uptake of AG337 because (1) absorptive permeabilities decreased as the concentration increased even though secretory permeabilities remained the same, (2) the absorptive transport rate was 37% lower in a medium containing verapamil and dipyridamole than in a medium containing only verapamil, and (3) the absorptive transport rate was also lower in a medium containing verapamil and a nucleobase mixture (consisting of adenine, hypoxanthine, and xanthine at 100 μM each) than in a medium containing verapamil only. Apical transport of AG337 in the Caco-2 cells is mediated, at least in part, by p-glycoprotein (efflux) and a nucleobase transporter that transports (uptake) nucleic bases.

Keywords: Uptake; efflux; activation energy; inhibitors; absorptive; secretory

Introduction

The test compound, 3,4-dihydro-2-amino-6-methyl-4-oxo-5-(4-pyridylthio)quinazoline dihydrochloride (AG337), is a lipophilic and nonclassical antifolate inhibitor of thymidylate synthase. AG337 represents a promising new class of anticancer agents that were designed on the basis of a three-dimensional structure of TS derived from X-ray crystallography.[1,2] It has been shown to inhibit the growth of various tumor cell lines by inhibiting the function of thymidylate synthase.[1] It is effective against im and ip implanted tumors in animals at an oral dose of 150 mg/kg twice daily.[1] The development of an efficient oral dosage form should further enhance the drug's therapeutic potentials.

Previously, we have showed that this compound is transported by a nucleobase transporter in the rat small intestine.[3] The transport of AG337 was shown to be concentration-, Na^+-, temperature-, and pH-dependent. Trans-

* To whom correspondence should be addressed: College of Pharmacy, Washington State University, Pullman, WA 99164-6534. Phone: (509) 335-4184. Fax: (509) 335-5902. E-mail: minghu@wsu.edu.

(1) Webber, S.; Bartlett, C. A.; Boritzki, T. J.; Hilliard, J. A.; Howland, E. F.; Johnston, A. L.; Kosa, M.; Margosiak, S. A.; Morse, C. A.; Shetty, B. V. AG337, a novel lipophilic thymidylate synthase inhibitor: in vitro and in vivo preclinical studies. *Cancer Chemother. Pharmacol.* **1996**, *37*, 509−517.

(2) Clendeninn, N. J.; Johnston, A. Phase II trials of Thymitag™ (AG337) in six solid tumor diseases. *Proc. Am. Assoc. Cancer Res.* **1996**, *37*, 86 (abstract 296).

10.1021/mp034012d CCC: $27.50
Published on Web 03/31/2004

port was also inhibited 80% by pyrimidine base mixtures containing adenine, hypoxanthine, and xanthine at 100 μM each, but not by a mixture of thymine and uracil at 100 μM each. In addition, a mixture containing the first three nucleobases at 100 μM each was more effective than thymine and uracil at 1000 μM each. The intestinal wall permeability was high (approximately 4), indicating the drug is expected to be absorbed well in humans according to a published correlation using the same method.[4]

The purpose of this study is to determine the transepithelial transport mechanism of AG337 in a Caco-2 cell culture system. Although the bulk of our study was done using Caco-2 TC7 clones, we also determined if different clones of Caco-2 cells will significantly affect the transport of AG337. There is currently one published report of nucleobase transport in the Caco-2 model in which the transport of uracil was studied.[5] Previously, we have shown that uracil did not affect transport of AG337 in the rat intestine.

The Caco-2 cell culture system is routinely used as a model for studying the intestinal absorption mechanism of drugs, for determining a drug candidate's absorption potential, and for studying the metabolism of drugs.[6−8] This human intestinal model system is very well suited for the current study since the purpose of this study is to determine the kinetic characteristics of transepithelial transport in both absorptive and secretory directions.

Materials and Methods

Materials. AG337 was provided by Agouron Pharmaceuticals (La Jolla, CA). Adenine, hypoxanthine, xanthine, verapamil, dipyridamole, probenecid, and other chemicals were purchased from Sigma (St. Louis, MO). Structures of AG337 and nucleobases are shown in ref 3.

Cell Culture. Caco-2 cells are routinely grown in our laboratories for more than 10 years. Three variants of Caco-2 cells were used in this study. The first one is the Caco-2 TC7 clone (denoted TC7) obtained from INSERM of France, and was a gift of M. Rousset of INSERM U178 (Villejuit, France). The second one (Caco-2 wild type, denoted ATCC) originated from the University of Kansas (Lawrence, KS), and was a gift of R. T. Borchardt. The third one (Caco-2CMV3A4, clone 4) was previously obtained from GENTEST Corp. (Woburn, MA). Cells were seeded to Millicell-PCS inserts at a density of 200 000 cells/insert (surface area of 4.2 cm^2) and grown for the appropriate period of time. Caco-2 TC7 cells were grown using 15% fetal bovine serum (FBS) unless otherwise specified, whereas wild-type Caco-2 and Caco-2CMV3A4 cells were grown in 10% FBS. Caco-2 TC7 cells (passage 15−29) were used between 18 and 22 days postseeding. Wild-type Caco-2 cells (passage 82) were grown for a similar period of time before being used. Caco-2CMV3A4-clone 4 cells were used approximately 13−15 days postseeding because they grow faster.

Preparation of Monolayers for Experiments. At the date of the experiment, cell monolayers were removed from the incubator, and the growth medium was aspirated out. After addition of 4.5 mL of HBSS (pH7.4) to each monolayer (2.5 mL outside and 2 mL inside), the transepithelial electrical resistances were measured using a Millicell-ERS instrument (Millipore Corp., Bedford, MA). The monolayers were incubated with the buffer for 1 h at 37 °C before being used.

Transport Experiments. The majority of the experiments investigating the characteristics of p-glycoprotein (p-gp) were performed as vectorial transport studies where apical to basolateral (A−B) and basolateral to apical (B−A) transport were assessed simultaneously. A smaller number of studies focused on an absorption (A−B transport) mechanism that involved a nucleobase transporter.

Experimental Protocol. Standard transport experiments were performed in a shaking incubator (Newbrunswick G-24) using an orbital shaking speed of 50 rpm. When the diffusion chamber was used for the experiment (see ref 8 or 13 for

(3) Hu, M.; Roland, K.; Ge, L.; Chen, J.; Tyle, P.; Roy, S. Determination of Absorption Characteristics of AG337, a Novel Thymidylase Synthase Inhibitor, Using a Perfused Rat Intestinal Model. *J. Pharm. Sci.* **1998**, *87*, 886−890.

(4) Amidon, G. L.; Sinko, P. J.; Fleisher, D. Estimating human oral fraction dose absorbed: a correlation using rat intestinal membrane permeability for passive and carrier-mediated compounds. *Pharm. Res.* **1988**, *5*, 651−654.

(5) Li, H.; Chung, S. J.; Shim, C. K. Characterization of the transport of uracil across Caco-2 and LLC-PK1 cell monolayers. *Pharm. Res.* **2002**, *19*, 1495−1501.

(6) Artursson, P.; Karlsson, J. Correlation between oral drug absorption in humans and apparent drug permeability coefficients in human intestinal epithelial (Caco-2) cells. *Biochem. Biophys. Res. Commun.* **1991**, *175*, 880−885.

(7) Gan, L. S. L.; Moseley, M. A.; Khosla, B.; Augustijns, P. F.; Bradshaw, T. P.; Hendren, R. W.; Thakker, D. R. CYP3A-like cytochrome p-450-mediated metabolism and polarized efflux of cyclosporin A in Caco-2 cells: Interaction between the two biochemical barriers to intestinal transport. *Drug Metab. Dispos.* **1996**, *24*, 344−349.

(8) Hu, M.; Zheng, L.; Chen, J.; Liu, L.; Zhu, Y.; Dantzig, A. H.; Stratford, R. E., Jr. Mechanisms of Transport of Quinapril in Caco-2 Cell Monolayers: Comparison with Cephalexin. *Pharm. Res.* **1995**, *12*, 1120−1125.

(9) Augustijins, P. J.; Bradshaw, T. P.; Gan, L. S. L.; Henden, R. W.; Thakker, D. R. Evidence for a polarized efflux system in Caco-2 cells capable of modulating cyclosporin A transport. *Biochem. Biophys. Res. Commun.* **1993**, *197*, 360−365.

(10) Hunter, J.; Hirst, B. H.; Simmons, N. L. Drug absorption limited by p-glycoprotein-mediated secretory drug transport in human intestinal epithelial Caco-2 cell layers. *Pharm. Res.* **1993**, *10*, 743−749.

(11) Burton, P. S.; Conradi, R. A.; Hilgers, A. H.; Ho, N. F. H. Evidence for a polarized efflux system for peptides in the apical membrane of Caco-2 cells. *Biochem. Biophys. Res. Commun.* **1993**, *190*, 760−766.

(12) Hosoya, K. I.; Kim, K. J.; Lee, V. H. L. Age-dependent expression of p-glycoprotein gp170 in Caco-2 cell monolayers. *Pharm. Res.* **1996**, *13*, 885−890.

(13) Hu, M.; Chen, J.; Tran, D.; Zhu, Y.; Leonardo, G. The Caco-2 cell monolayers as an intestinal metabolism model: Metabolism of dipeptide Phe-Pro. *J. Drug Targeting* **1994**, *2*, 78−89.

details of the chamber method), the rate of stirring is 300 rpm. The experiments were performed at 37 °C unless otherwise specified. The donor pH was typically 6.5, and the receiver pH was typically 7.4 unless specified otherwise. Briefly, following the incubation of monolayers with HBSS, the incubation buffer was removed; a pH 6.5 HBSS buffer supplemented with 25 mM MES was loaded onto the donor side, and the amount transported to the receiver side was monitored as a function of time by HPLC. Four samples were taken from the AP side, and two were from the donor side. The recovery was calculated at the end of experiments. The typical recovery ranged from 85 to 115%, indicating insignificant metabolism, degradation, or adsorption to the experimental apparatus.

HPLC Analysis. The concentration of AG337 was analyzed via HPLC after centrifugation of samples at 4500 rpm for 30 min. The HPLC conditions were as follows: H-P 1090 Series II HPLC system with a diode array detector, a Beckman Ultrasphere analytical column (particle size of 5 μm and dimensions of 4 mm × 250 mm), mobile phase of 48% 24 mM NaH_2PO_4, 32% 16 mM $NH_4H_2PO_4$, 10% CH_3OH, and 10% CH_3CN with the pH adjusted to 3 after mixing, wavelength of 273 nm, flow rate of 1 mL/min, injection volume of 50 μL, and tested linear range of 1.25−20 μM.

Data Analysis. Rates of transport (B_t) were obtained using the concentration of transported AG337 as a function of time (eq 1). Permeability (P) across a cellular membrane was calculated using the rate of transport divided by the surface area (A) of the monolayer and the initial concentration of AG337 at the loading side (C_i) (eq 2).

$$B_t = \frac{dC}{dt} xV \quad (1)$$

$$P = \frac{B_t}{AC_i} \quad (2)$$

Statistical Analysis. A one-way ANOVA or Student's *t*-test was used to analyze the data. The prior level of significance was set at 5% or $p < 0.05$.

Results

Vectorial Transport of AG337. Amounts of AG337 that were transported always increased linearly with time (Figure 1). In the absence of p-gp inhibitors, the level of basolateral to apical (B−A) or secretory transport of AG337 was always higher ($P < 0.01$) than the level of apical to basolateral (A−B) or absorptive transport (Figure 1 and Table 1). At a concentration of 25 μM, the B−A/A−B transport ratio was approximately 10 (Table 1).

The vectorial transport of AG337 (25 μM) was more pronounced in the Caco-2 TC7 clone than in wide-type ATCC cells (Figure 1). In Caco-2CMV3A4-clone 4 cells, which were shown to express human CYP3A4, the B−A/A−B transport ratio was ~2.2 with an A−B transport rate of 9.76 ± 1.43 pmol min^{-1} cm^{-2} and a B−A rate of 21.9 ± 0.2 pmol min^{-1} cm^{-2}. This A−B rate was 589% faster than the A−B rate in the TC7 cells (1.43 ± 0.12 pmol min^{-1} cm^{-2}, Table 1) but was only 50% faster than the B−A rate in the TC7 cells (14.7 ± 0.6 pmol min^{-1} cm^{-2}, Table 1).

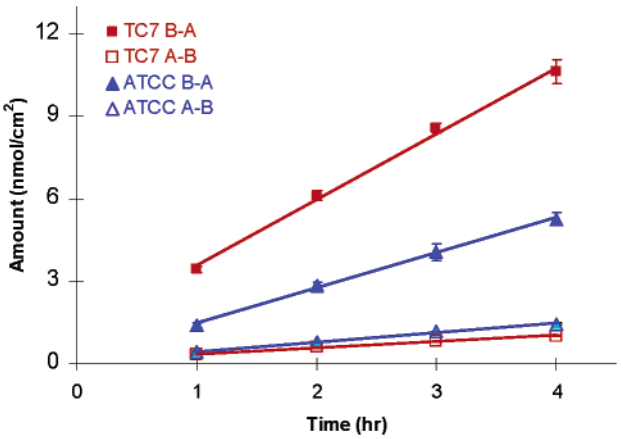

Figure 1. Vectorial transport of AG337 in Caco-2 cells. Transport of 25 μM AG337 in wild-type (ATCC, triangles) and cloned (TC7, squares) Caco-2 cells was assessed as a function of time (hours) at 37 °C in both the absorptive direction (A−B, filled symbols) and the secretory direction (B−A, empty symbols). The donor buffer was pH 6.5 MES HBSS, and the receiver buffer was pH 7.4 HBSS. Each data point is the average of three determinations, and the error bars represent the standard deviation of the mean.

Table 1. Effect of Concentration on the Transepithelial Transport of AG337[a]

concentration (μM)	rate of transport (pmol min^{-1} cm^{-2}) A−B (mean ± SD)	B−A (mean ± SD)	ratio
10	1.88 ± 0.69	14.1 ± 0.05	7.6
25	3.79 ± 0.24	40.0 ± 4.29	10.6
50	6.33 ± 0.55	93.3 ± 4.76	14.7
75	7.74 ± 0.21	132.9 ± 1.05	17.2
100	9.60 ± 0.71	197.1 ± 14.76	20.5
150	13.83 ± 0.50	232.6 ± 4.05	16.8

[a] Experiments were performed at 37 °C for 4 h. Donor and receiver volumes were 3 mL. The rate was calculated from the slope of the amount transported vs time curve.

Since TC7 cells were fed with 15% FBS whereas the ATCC cells were fed with 10% FBS, we also tested the effect of the FBS concentration on the transport of AG337. The results indicated that an increase in the percentage of FBS increased the absorptive rate and permeability and the FBS effects were much more pronounced on the absorptive transport than on the secretory transport (Figure 2).

Effect of Stirring Rate on the Transport of AG337. Transport rates and permeabilities of AG337 were enhanced when a more rigorous stirring was used in a diffusion chamber (Figure 3). The effect is approximately equal in both directions (enhanced ≈3.5 times), with a slight effect on the A−B/B−A transport ratio (which remained at 10-fold at an AG337 concentration of 25 μM). Since the donor concentration used in many subsequent experiments was low (e.g., 10 μM), we have selected the shaker method. The

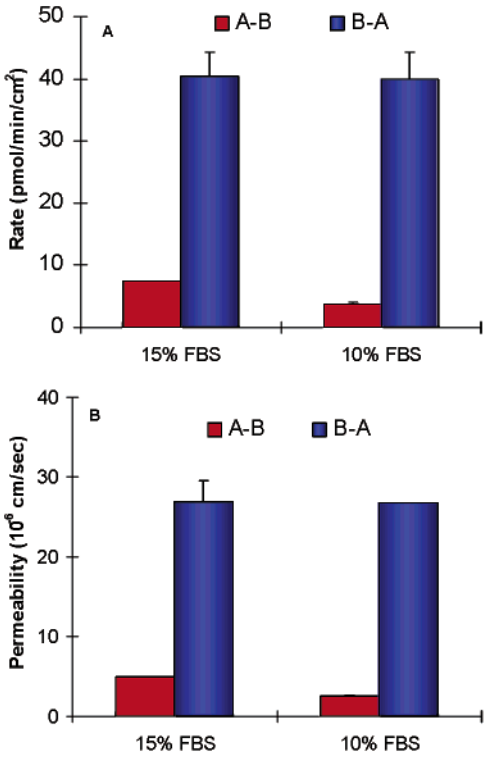

Figure 2. Effect of serum concentration on transport of AG337 in TC7 cells. The concentration of AG337 was 10 μM, and experiments were carried out for 2−4 h at 37 °C. The donor buffer was pH 6.5 MES HBSS, and the receiver buffer was pH 7.4 HBSS. The rate of transport (A) and permeability (B) were determined using eqs 1 and 2 as described in Materials and Methods. Each data point is the average of three determinations, and the error bars represent the standard deviation of the mean.

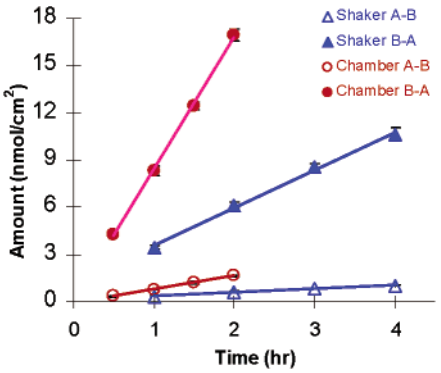

Figure 3. Effect of stirring intensity on the transport of AG337 using the Caco-2 TC7 cells. The concentration of AG337 was 10 μM, and experiments were carried out for 2−4 h at 37 °C. The donor buffer was pH 6.5 MES HBSS, and the receiver buffer was pH 7.4 HBSS. Each data point is the average of three determinations, and the error bars represent the standard deviation of the mean.

shaker method affords a higher surface area/volume ratio (2.2/1 vs 1/1.2). A higher ratio gave higher receiver drug concentrations, which help ensure the analytical reliability of the HPLC assay.

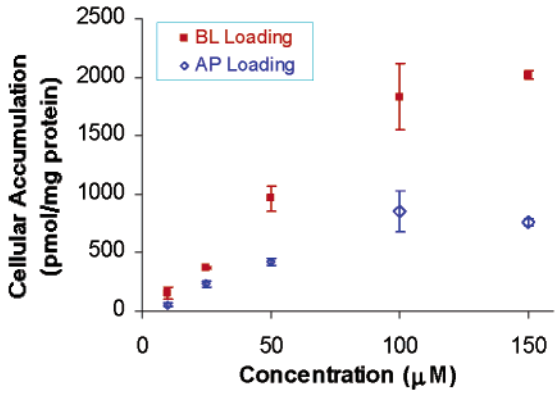

Figure 4. Effect of the concentration on the cellular accumulation of AG337. Experiments were performed over a 4 h period at 37 °C with apical loading (◇) or basolateral loading (■). The amounts that accumulated were measured after the cell monolayers were washed three times with an ice-cold saline solution. The donor buffer was pH 6.5 MES HBSS, and the receiver buffer was pH 7.4 HBSS. Each data point is the average of three determinations, and the error bars represent the standard deviation of the mean.

Effect of Concentration on the Transepithelial Transport of AG337. The rate of transepithelial transport of AG337 increased with an increase in concentration (Table 1). Although both A−B and B−A transport rates were increased, the rate of B−A transport was always higher (Table 1). The transport rate ratio (B−A/A−B) steadily increased as the concentration of AG337 increased from 10 to 100 μM, but fell slightly at a concentration of 150 μM (Table 1).

The kinetic parameters were not reported because evidence suggests the involvement of multiple carriers in the transepithelial transport of AG337. The other reason is that we could not (due to solubility limitation) increase the concentration of AG337 much beyond 150 μM to effect a near-complete saturation of the transporters that are involved.

Effect of Concentration on the Cellular Accumulation of AG337. Cellular accumulation of AG337 was assessed at concentrations of 10, 25, 50, 100, and 150 μM (Figure 4). The results showed that the level of accumulation increased with concentration until 100 μM, after which a further increase in the concentration did not result in an increase in the level of accumulation.

Effect of pH on the Transepithelial Transport of AG337. A−B transport of AG337 was measured with apical pHs of 5.5, 6.5, and 7.4 with the same basolateral pH of 7.4. The results indicated that the apical pH did not affect the A−B transport of AG337 (Figure 5).

Effect of Temperature on the Transepithelial Transport of AG337. The effect of temperature was studied using a concentration of 75 μM so that the amount of AG337 transported or taken up can be measured reliably at 4 °C. The rates of both A−B and B−A transport of AG337 (75 μM) decreased with temperature (from 37 to 4 °C, Figure 4). The apparent activation energy for the A−B transport was 34.8 kJ/mol or 8.3 kcal/mol. The effect of temperature

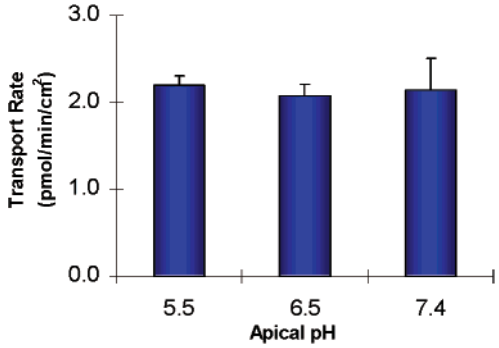

Figure 5. Effect of donor pH on the A−B transport of AG337 using TC7 cells. Experiments were performed over a 4 h period at 37 °C using 10 μM AG337. The donor buffer was varied from pH 5.5 to 7.4, and the receiver buffer was pH 7.4 HBSS. Each bar is the average of three determinations, and the error bars represent the standard deviation of the mean.

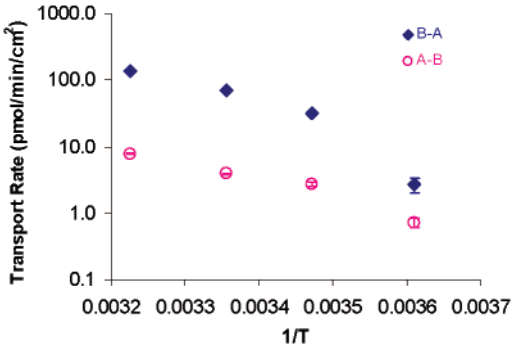

Figure 6. Effect of temperature on the transport of AG337 (Arrhenius plot) in Caco-2 TC7 cells. Rates of A−B transport (○) and B−A transport (◆) of AG337 are plotted vs the inverse temperature (expressed as inverse kelvin). The drug concentration was 75 μM, and the experiments were performed for 4 h at different temperatures. Each bar is the average of three determinations, and the error bars represent the standard deviation of the mean.

on the B−A transport was curved, with two apparent components. The first component was from 37 to 15 °C, where the apparent activation energy was 41 kJ/mol or 10 kcal/mol. This activation energy is not different from the A−B activation energy. The second component is from 15 to 4 °C, where the apparent activation energy was 140 kJ/mol or 35 kcal/mol.

Effect of Temperature on the Cellular Accumulation of AG337. The level of cellular accumulation of AG337 only changed modestly (<1-fold) with temperature for apical drug loading, but changed substantially (>7-fold) with temperature for basolateral loading (Figure 7). Concerned about the possibility that the drug may merely adsorb to the polycarbonate membrane, we incubated AG337 (75 μM) with polycarbonate membranes coated with rat collagen for 4 h at 4 °C, and measured the amount of AG337 associated with the membrane. The amount was less than 1% (i.e., considered negligible) of the amount that was found to be associated with the cell membrane when the drug was loaded basolaterally.

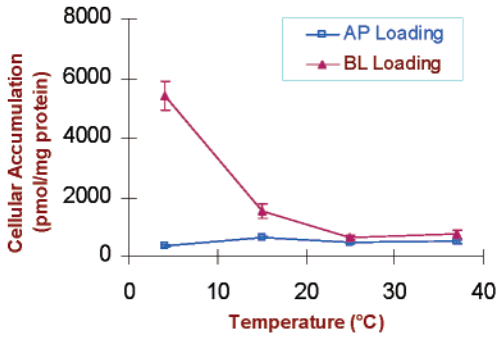

Figure 7. Effect of temperature on the cellular accumulation of AG337. The curve that represents basolateral loading is depicted with filled triangles. The curve that represents apical loading is depicted with empty squares. The drug concentration was 75 μM, and the experiments were performed for 4 h at different temperatures. Each bar is the average of three determinations, and the error bars represent the standard deviation of the mean.

Effect of Potential Inhibitors on the Transepithelial Transport of AG337. We used a variety of transport inhibitors to determine how they affect the transepithelial transport of AG337. The results indicated that inhibitors of p-gp (e.g., verapamil and dipyridamole) generally significantly ($p < 0.05$) increased the rate of A−B transport but decreased the rate of B−A transport (Table 2). On the other hand, the inhibitors of nucleobase transport (e.g., adenine, hypoxanthine, and xanthine) generally decreased ($p < 0.05$) the rate of A−B transport without affecting the rate of B−A transport. When both verapamil and a mixture of nucleobase were used, the rate of A−B transport of AG337 was higher than the rate of transport in the absence of any inhibitors but was lower than the rate of transport in the presence of verapamil only. Last, B−A transport of AG337 (50 μM) was inhibited 67% by 1000 μM verapamil, whereas A−B transport of AG337 was enhanced 67% by 1000 μM verapamil.

Effect of Potential Inhibitors on the Intracellular Accumulation of AG337. We assessed intracellular accumulations of AG337 in the presence of selected inhibitors (Table 3). The results indicated that drug accumulation was higher when the drug was loaded basolaterally than apically (see also Figure 2). Inhibitors of p-gp always increased the intracellular drug concentration to a higher level. Whereas the highest level of accumulation was achieved when AG337 was loaded basolaterally in the presence of inhibitors, a larger percentage increase (550%) was achieved when AG337 was loaded apically in the presence of inhibitors.

Discussion

In an earlier study in which the absorption of AG337 in the rat intestine was investigated, we found that the drug was transported at least partially by a nucleobase transporter(s).[3] In the study presented here, we determined the transport mechanisms of AG337 in the Caco-2 cell culture model and compared the results with what we obtained from the rat intestine.

Table 2. Effects of Potential Inhibitors on the Transepithelial Transport of AG337

inhibitor	concentration (μM)	rate of transport (pmol min^{-1} cm^{-2}) A−B (mean ± SD) (% control ± SD)	rate of transport (pmol min^{-1} cm^{-2}) B−A (mean ± SD) (% control ± SD)	ratio (B−A/A−B)
control	−	2.07 ± 0.14 (100 ± 6.9)	16.90 ± 1.95 (100 ± 11.5)	8.2
verapamil	100	6.88 ± 0.07[a] (332 ± 3.5)	6.26 ± 0.14[a] (37.0 ± 0.85)	0.9
dipyridamole	10	2.93 ± 0.14[a] (141 ± 6.9)	11.05 ± 0.19[a] (65.4 ± 1.1)	3.8
verapamil and dipyridamole	100 and 10	4.36 ± 0.07[a,b] (210 ± 3.5)	6.52 ± 0.45[a] (38.6 ± 2.7)	1.5
A+H+X[c]	100 each	1.38 ± 0.05[a] (66.7 ± 2.3)	ND	N/A
verapamil and A+H+X	100 each	5.93 ± 0.33[a,b] (286 ± 16.1)	7.38 ± 0.29[a] (43.7 ± 1.7)	1.2
probenecid	10	1.67 ± 0.33 (80.5 ± 16.1)	15.79 ± 0.74 (93.4 ± 4.4)	9.5

[a] The difference between the control (no inhibitor) and the treatment is statistically significant ($p < 0.05$). [b] The difference between treatment with one chemical and treatment with two chemicals is statistically significant. [c] Adenine, hypoxanthine, and xanthine.

Table 3. Intracellular Accumulation of AG337 in the Presence of Inhibitors

inhibitor	concentration (μM)	amount accumulated (pmol/mg of protein) A−B (mean ± SD) (% control ± SD)	amount accumulated (pmol/mg of protein) B−A (mean ± SD) (% control ± SD)	ratio (B−A/A−B)
control	−	54 ± 13 (100 ± 24)	157 ± 50 (100 ± 32)	2.9
dipyridamole	10	196 ± 41[a] (363 ± 76)	442 ± 4[a] (282 ± 3)	2.3
dipyridamole and verapamil	10 and 100	296 ± 64[a] (548 ± 119)	447 ± 46[a] (285 ± 29)	1.5

[a] The difference between the control (no inhibitor) and the treatment is statistically significant ($p < 0.05$).

The results of our studies clearly demonstrate the presence of vectorial transport of AG337 in Caco-2 cell monolayers, regardless of which "clone" of the Caco-2 cells was used (Figures 1−3 and Tables 1 and 2). This vectorial transport was due to the presence of an efflux carrier at the apical surface that favors secretory transport and inhibits absorptive (A−B) transport. As a result, the rate of secretory transport at all the concentrations that were tested was higher ($p < 0.01$) than the rate of A−B transport (Table 1). Additional results in support of the presence of an apically located efflux carrier came from the effects of temperature on transport (Figure 6) and cellular accumulation. Secretory transport has a much higher activation energy (≈40 kcal/mol, 4−15 °C) than absorptive transport (≈8 kcal/mol, 4−15 °C) (Figure 6). This result suggests that secretory transport is an active process since an activation energy of ≥20 kcal/mol is typically associated with active transport. On the other hand, absorptive transport of AG337 at this concentration (75 μM) was probably mediated by passive diffusion since there was a slow increase in rate of absorptive transport at concentrations higher than 50 μM (Table 1). In addition, the level of cellular accumulation of AG337 decreased much more with temperature (decrease) when it is loaded basolaterally than when it is loaded apically (Figure 7). The latter suggests that the rate of apical efflux was decreased much more rapidly than the rate of basolateral uptake because the apical efflux carrier relies on the expenditure of cellular energy. Hence, at a lower temperature, there was a surge in intracellular accumulation. Taken together, these results suggest that an active component is involved in secretory transport of AG337 at the apical membrane.

To determine which carriers may be involved in the apical uptake and efflux of AG337, a variety of inhibitors were used. The first group is inhibitors of p-gp, and the second group is the inhibitors of nucleobase transporters. In the presence of various p-gp inhibitors (Table 2), the difference between absorptive transport and secretory transport became smaller (in the case of dipyridamole or a mixture of verapamil and dipyridamole), or disappeared completely (in the case of 100 μM verapamil). Since verapamil is a prototypical inhibitor of p-gp, AG337 is likely a substrate of p-gp. Other studies of AG337 in Caco-2 cells also support the role played by p-gp. For example, intracellular accumulation of AG337 was enhanced by the use of p-gp inhibitors such as verapamil and dipyridamole (Table 3). Because p-gp is known to have the capability of extracting substrate from the cellular membrane (i.e., before it enters the cytosolic domain),[14] it could explain why the level of intracellular accumulation was always higher when p-gp is loaded basolaterally instead of apically. Therefore, p-gp is likely to be the transporter responsible for the efflux of AG337 at the apical membrane of the Caco-2 cells.

If p-gp were the only transporter involved in the transepithelial transport of AG337, then we would not expect to produce a secretory/absorptive transport ratio that increased as the concentration increased (Table 1). This is because an increase in the concentration generally does not affect passive diffusion, but may lead to saturation of p-gp. Saturation of p-gp generally leads to an increase in the rate of absorptive transport and a decrease in the rate of secretory transport, which will then lead to a decrease in the secretory/absorptive transport ratio. Therefore, it is likely that a process in addition to passive diffusion was involved in the uptake of drugs by Caco-2 cells (see the discussion below).

(14) Gottesman, M. M.; Pastan, I.; Ambudkar, S. V. P-glycoprotein and multidrug resistance. *Curr. Opin. Genet. Dev.* **1996**, *6*, 610−617.

The results indicated that the nucleobase transporter(s) was also involved in the absorptive transport of AG337, but not in the secretory transport of AG337. Results in support of this hypothesis include the following. The rate of absorptive transport of AG337 (in the presence or absence of verapamil) always decreased in the presence of adenine, xanthine, and hypoxanthine (100 μM each), whereas B−A transport of AG337 was not affected. The inhibitor cocktail (adenine, xanthine, and hypoxanthine at 100 μM each) is a mixture of purine nucleobases previously shown to inhibit (by 80%) transport of AG337 in the rat intestine. The involvement of an apically located carrier for uptake is further supported by the fact that an increase in the concentration of AG337, while increasing the rate of transport, did not lead to a proportional increase in the transport rates. Further characterization of the nucleobase transporters was not attempted here since the presence of p-gp could potentially dominate the transport kinetics of AG337 at the apical membrane, making it impossible to precisely sort out the contribution of the nucleobase transporter. Last, AG337 appears to enter the basolateral membrane of the cells via passive diffusion since a mixture of three nucleobases shown to inhibit apical uptake and accumulation did not result in a further decrease in the rate of secretory transport of AG337.

Finally, in the experiments we performed using transfected Caco-2 cells (which express human CYP3A4 activity that is 20−40 times higher than that in normal TC7 cells),[15,16] the ratio of secretory rate to absorptive rate was smaller than that in the TC7 Caco-2 cells (at 10 μM). These results suggest that the functional activity of p-glycoprotein did not increase. The decrease in the ratio was primarily due to an increase in A−B permeability. This is not surprising since CYP3A4-expressing cells reached maturity earlier than nontransfected Caco-2 cells, which could in turn lead to an increased rate of transport of nucleobases. In our earlier investigation, the CYP3A4-expressing cells also had increased rates of uptake of amino acids when compared to wild-type ATCC cells.[17] Our data are consistent with the earlier observation that more expression of p-gp is not necessarily associated with higher CYP3A4 activity.[16] This result provided another evidence that the expression of p-gp is not necessarily associated with the expression of CYP3A4 in this cell type as observed by Cummins et al.[16] This is not entirely surprising since the increases in CYP3A4 activities in the transfected Caco-2 cells were driven by a CMV promoter, not normally involved in the regulation of CYP3A4 and p-gp in the Caco-2 cells. Moreover, previous studies have shown a lack of coordinate expression in liver.[18] Nevertheless, when a chemical such as 1α,25-dihydroxyvitamin D_3 is used, it can effect the regulation of both CYP3A4 and p-gp because it is an effective regulator of both proteins.[19] Taken together, the current study indicated that an increase in the level of expression of CYP3A4 will not necessarily cause an increase in the level of expression of p-gp.

In conclusion, apical transport of AG337 is mediated by passive diffusion, nucleobase transporter, and p-gp, whereas basolateral transport appeared to be mediated by passive diffusion only. The two active transport mechanisms work against each other at the apical membrane to confer unique characteristics to the transport of AG337 in the Caco-2 cells.

Acknowledgment. Work supported by Agouron Pharmaceutical and National Institutes of Health Grant GM52270. We thank Ms. Yiqi Li for her technical assistance.

MP034012D

(15) Crespi, C. L.; Penman, B. W.; Hu, M. The Development of Caco-2 Cells Expressing High Levels of cDNA-Derived Cytochrome P4503A4. *Pharm. Res.* **1996**, *13*, 1635−1641.

(16) Cummins, C. L.; Mangravite, L. M.; Benet, L. Z. Characterizing the expression of CYP3A4 and efflux transporters (P-gp, MRP1, and MRP2) in CYP3A4-transfected Caco-2 cells after induction with sodium butyrate and the phorbol ester 12-*O*-tetradecanoylphorbol-13-acetate. *Pharm. Res.* **2001**, *18*, 1102−1109.

(17) Hu, M.; Li, Y.; Davitt, C. M.; Huang, S. M.; Thummel, K.; Penman, B. W.; Crespi, C. L. Transport and metabolic characterization of Caco-2 cells expressing CYP3A4 and CYP3A4 plus oxidoreductase. *Pharm. Res.* **1999**, *16*, 1352−1359.

(18) Salphati, L.; Benet, L. Z. Modulation of P-glycoprotein expression by cytochrome P450 3A inducers in male and female rat livers. *Biochem. Pharmacol.* **1998**, *55*, 387−395.

(19) Schmiedlin, R. P.; Thummel, K. E.; Fisher, J. M.; Paine, M. F.; Lown, K. S.; Watkins, P. B. Expression of enzymatically active CYP3A4 by Caco-2 cells grown on extracellular matrix-coated permeable supports in the presence of 1α,25-dihydroxyvitamin D3. *Mol. Pharmacol.* **1997**, *51*, 741−754.